JOURNAL OF APPLIED ELECTROCHEMISTRY 18 (1988) 839–848

Electrochemistry of anodic F_2 evolution at carbon electrodes: bubble adherence effects in the kinetics at rotating cone electrodes

LIJUN BAI, B. E. CONWAY

Chemistry Department, University of Ottawa, 32 George Glinski Street, Ottawa, K1N 9B4 Canada

Received 3 October 1987; revised 1 April 1988

Fluorine-evolving carbon anodes exhibit unusually high overvoltages characterized also by remarkably large Tafel slopes having values 0.4–0.8 V per decade of current density change. Also, at high current densities, a so-called 'anode effect' associated with a type of passivation sets in. Experiments are described which aim to distinguish high polarization arising from an intrinsically large Tafel slope, generated by a non-ohmic charge transfer barrier layer effect due to 'CF' film formation, from effects due to difficulties of F_2 bubble detachment and F_2 gas film formation at the 'CF' film. Steady state polarization measurements have been made at a rotating carbon cone electrode from which F_2 bubbles, which otherwise remain attached to the electrode and block access to the electrolyte, can be spun away. At the rotated electrode, at low and intermediate current densities, linear Tafel behaviour is still observed but with high slopes associated with the barrier layer film effect. At higher current densities an 'anode effect', associated with the F_2 gas film, is developed, leading to a type of passivation of the electrode. The two sources of unusually high polarization in the F_2 evolution reaction at carbon are not independent as it is also the formation of the 'CF' film that causes difficulties in gas bubble detachment owing to the lyophobic properties of the fluorinated $C/F_2/KF \cdot 2HF$ interface. Polishing effects confirm this conclusion.

1. Introduction

The anodic fluorine evolution reaction (FER) at carbon electrodes in $KF \cdot 2HF$ melts is a complex process and the conditions under which the FER proceeds lead to difficulties for kinetic studies of the reaction. Porous carbon electrodes are used on which an electrolytically generated 'CF' film exists [1, 2] arising either from oxidation of the C by F or from intercalation (in the case of graphite). This film gives rise to a very low surface energy and an unusually high solid/gas/liquid contact angle [3, 4] which makes F_2 bubble formation on, and detachment from the electrode surface a serious problem both in the F_2 production industry and in laboratory kinetic and mechanistic experiments. Under either of the latter conditions, a so-called 'anode effect' has been recognized [3, 4] and is characterized by a sudden increase of cell voltage and an accompanying decrease of current when electrolysis was previously proceeding at high current density. On account of this problem, discrepant results and controversial conclusions have not surprisingly been reported [5–7] with regard to the Tafel polarization behaviour. Also, controversial results from interfacial capacitance measurements have arisen, connected with unusual ohmic iR drop behaviour [8].

While, formally, the electrode kinetic behaviour of the FER might be expected to follow that for Cl_2 or H_2 formation, with consecutive ion discharge and desorption/recombination steps [9] exhibiting Tafel slopes of *ca* 0.12, 0.04 or 0.029 V (at 298 K), the anodic evolution of F_2 at C is associated with remarkably high Tafel slopes of 0.4–0.8 V (at *ca* 358 K). Such values can arise from charge transfer across non-ohmic barrier layer films (as at the valve metals [10]), as was noted in an earlier publication [7] related to this project.

Under both industrial [11] and laboratory [4] conditions, F_2 is evolved from $KF \cdot 2HF$ melts as strongly adherent bubbles of lenticular form which are sluggish in their detachment from the electrode. In fact, the electrode takes on a mirror-like appearance originating from total internal reflection at an extended F_2 bubble/electrolyte interface at the electrode surface and, when these conditions obtain, high polarization* results.

Determination of the origin of the high Tafel slopes for anodic F_2 evolution at C is important practically with regard to electric energy consumption and is also of theoretical interest [7, 11].

The relation of F_2 bubble behaviour to the high polarization at C, especially the 'anode effect' was studied by Watanabe *et al.* [4, 12] who proposed that

* Note that the bubble polarization effect referred to here is quite different from that suggested in classical overvoltage literature where bubble nucleation was envisaged as the origin of overvoltage; nor is the present effect related to supersaturation prior to bubble evolution, envisaged as a possible origin of pseudo-polarization effects, e.g. in cathodic H_2 evolution at active Pt electrodes. Effects arising from changes of effective resistivity of the electrolyte, due to suspension of dispersed small bubbles, are also known but do not arise here since the form of the bubbles is quite different.

0021-891X/88 $03.00 + .12

an F_2 gas film is established on the surface due to formation of a solid 'CF' film having a low surface free energy. The gas film diminishes the available electrochemically active area of the electrode. However, the barrier effect of a non-ohmically conducting 'CF' film for electron transfer was not considered in Watanabe's model which cannot explain the observed linear Tafel relation with unusually high slope (*ca* 0.4 V) over 3–4 decades of current change (see below, Fig. 7) already beginning at a potential of 4 V where there is no observable F_2 bubble formation. (F_2 may be transported into the melt or inside the pores of the electrode, or both.)

It was concluded in work by Brown *et al.* [15] that, for most of the time, 99% of vitreous C or graphite anode surfaces was blocked by an F_2 gas bubble film but the bubble 'overvoltage' effect,* he supposed, could be avoided by a potential step polarization procedure.

A contrary view, that the high Tafel slope was, in fact due to 'CF' barrier film effect, was expressed by Devilliers *et al.* [13, 14] in terms of the barrier height and modified by Brown *et al.* [15] in terms of barrier width. The onset of the anode effect was attributed by Devilliers *et al.* to development of an excessively thick 'CF' film but this does not seem to be supported by surface analysis experiments [15, 16]. However, practically important high current densities ($\geqslant 0.1\,A\,cm^{-2}$), where the bubble effect arises, were avoided in their work.

In other work [1–3, 14–16] it has been found by ESCA [15, 16] that 'CF' films of 10–30 Å are already almost completely formed at *ca* 2 V (a kind of UPD of F at C) even before steady currents for F_2 evolution can arise and the film thickness does not further increase significantly with electrode potential. In fact, there is no direct evidence that the 'anode effect' is caused by formation of a thicker, less-conducting 'CF' film since such a 'CF' film already exists at much lower overvoltages.

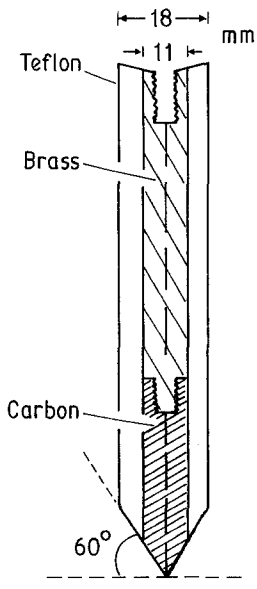

Fig. 1. Diagram of the rotating carbon cone electrode (RCE).

* See footnote of previous page.

In the light of the previous literature, the present work is therefore directed at distinguishing polarization effects that can arise from gas film formation and difficulty in bubble detachment, from other sources, principally that arising from activated charge transfer across a non-ohmically conducting 'CF' film. By means of a rotating cone electrode (RCE), unlike the situation at a rotating disc electrode (RDE), F_2 bubbles can be spun up and off the electrode, enabling the bubble effect to be minimized and thence other sources of polarization to be better evaluated. The quantitative hydrodynamic mass transfer behaviour [19] at the RCE will not concern us in this aspect of the work; rather, the geometry of the acute angled (60°) cone provides an upward and radial flow across the surface of the RCE which facilitates removal of adherent bubbles at the surface boundary layer.

2. Experimental details

2.1. *Cell*

A cylindrical cell (volume 500 cm^3), constructed from Plexiglass, was used to contain the KF · 2HF melt at the 358 K temperature employed in the work. The cell was made from Plexiglass rather than Teflon in order that development of F_2 bubbles on the working C electrode could be visually observed and photographically recorded. The cathode was mounted in a cylindrical compartment, allowing separation of evolved H_2 from the anode.

2.2. *Rotating fluorine anode*

A rotating carbon cone electrode (RCE) was used, the purpose being to facilitate F_2 bubble detachment and removal by rotation. Conical geometry is required since, at an RDE, a recumbent gas bubble resides at the flat electrode interface, even at high rotation speeds, and eventually cuts down the current to a few $mA\,cm^{-2}$. By contrast, at Pt RDEs evolving H_2, no bubble problem arises right up to high current densities [18] indicating that, with F_2 at carbon, the difficulty arises because of bubble adherence due to an unfavourable contact angle. Contrary to the behaviour at the RDE, at a carbon RCE we find that bubble detachment is strongly facilitated so that the bubble effect could be largely eliminated (see below) or greatly reduced by rotation.

The RCE was fabricated and mounted in Teflon (Fig. 1), coupled with a mandrel that could be spun in a Pine Instrument Co. (Grove City, PA, USA) electrode rotator. The cone was cut from porous carbon of the kind used in commercial F_2 production (supplied by Sers Savoie Carbone, France [7, 11]) and machined at a 60° angle, and gave an apparent surface area of 1.73 cm^2. Several RCEs of identical geometry were made and reproducibility of results was checked and confirmed by performing measurements successively on the different RCEs.

Some carbon RCEs were polished by the procedure

described in a patent [11] granted to Eldorado. Briefly, the procedure consists in polishing the carbon anode surface with a series of grit sandpapers and then with diamond polishing compounds, finishing with a polish using 0.25 μ abrasive; the main resulting difference is that the polished carbon anodes have a much smoother surface as revealed by scanning electron microscopy.

2.3. *Counter electrode (cathode)*

The cathode was 0.25 cm diameter rod of mild steel (as used in industrial cells), giving about 7.5 cm^2 surface area exposed to the melt.

2.4. *Reference electrodes*

Four identically prepared Cu/CuF_2 reference electrodes were used in the KF · 2HF melt at 358 K, as in other works [20, 21], and behaved satisfactorily. They were periodically checked against each other and against freshly prepared CuF_2 electrodes. Their stability was better than that attainable with $Pt(H_2)$ or Pd(H) in this melt [22, 23].

2.5. *Electrolyte melt*

Anhydrous KF · 2HF melts (supplied from Eldorado's Laboratory), prepared by dissolving KF in liquid HF with provision of cooling to absorb the heat of dissolution, were used in all experiments after pre-electrolysis at 2.5 V for 15 h at a sacrificial C electrode.

2.6. *Thermostatting*

The cell was mounted in an air-heated oven, operating as a thermostat ($\pm$0.5 K) controlled at 358 K. In this way contamination of the melt from corrosion of any internal heating coils or from a liquid thermostat fluid was avoided.

2.7. *Ohmic iR correction measurements*

All polarization results were corrected for *iR* drop, taking account of the special problems that arise [8] when the interfacial capacitance is unusually small, as is the case here due to the 'CF' film. *iR* drop measurements were made by the current interruption procedure [8, 24] and checked by a.c. impedance determinations [25]; results were in good agreement. The uncompensated solution resistances were 1.0–2.5 Ω for the KF · 2HF melt (358 K), depending on the geometrical arrangement of the electrodes in the cell.

2.8. *'On-line' data acquisition system for polarization measurements*

The steady state polarization data were acquired by an on-line computer system, which consisted principally of an HP-217 microcomputer with a Keithley 195A Digital Multimeter, a KEPCO Digital Programmer and a PAR 173 potentiostat. This system enabled the steady state polarization behaviour at the carbon anodes to be studied systematically under well-defined and reproducible conditions. Furthermore, the analysis of the results could be based on a large number of experimental data points measured and digitally recorded by the data acquisition system.

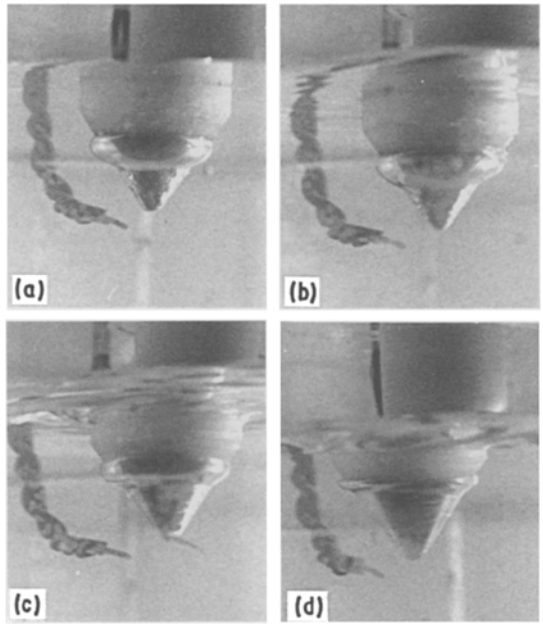

Fig. 2. Photographs of the normal (unpolished) RCE in the cell as polarized at 0.1 A cm^{-2} and rotated at: (a) 0 r.p.m. (stationary), showing the full size of a bubble on RCE; (b) 1000 r.p.m.; (c) 2500 r.p.m.; (d) 3600 r.p.m., showing the bubble is spun away from RCE surface.

2.9. *Reproducibility*

The results obtained at relatively high rotation rates ($\geqslant$ 2000 r.p.m.) were excellently reproducible. Ideally, the V vs log i Tafel plots for both the ascending and descending directions of potential change should be coincident for a reaction in a series of steady states (except when passivation arises). The V vs log i plots were monitored and displayed on a graphics screen during the actual sequence of measurements which were repeated until the ascending and descending plots had become almost coincident.

3. Results and discussion

3.1. *Illustration of F_2 bubble adherence at a carbon RCE*

Unlike the formation of H_2 bubbles at, e.g. iron cathodes, F_2 bubbles adhere strongly to the surface of carbon electrodes and form a visible extended bubble film covering most of the area of the RCE (see Fig. 2). The size of the bubble is increased with continuing passage of current and detachment of it eventually takes place when sufficient buoyancy forces develop as more F_2 accumulates in the bubble.

Figure 2a shows the full size of a bubble on the stationary RCE (0 r.p.m.). Figures 2b, c and d show

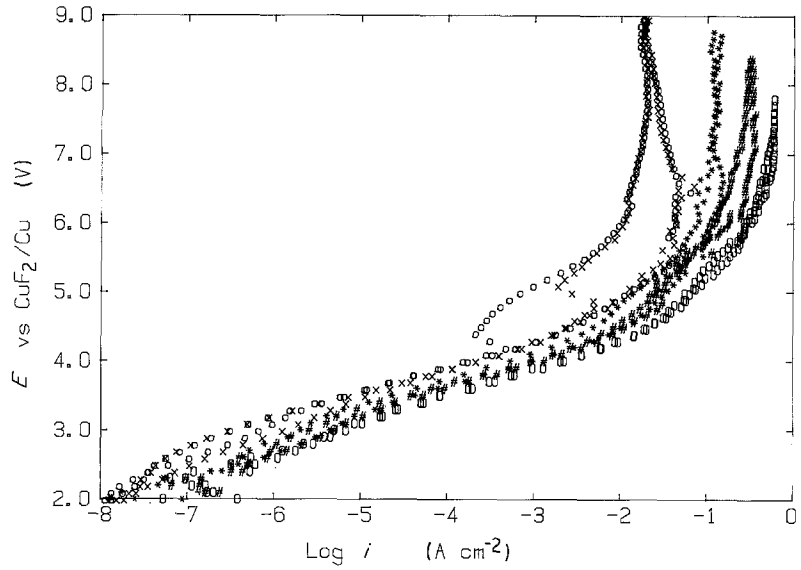

Fig. 3. Tafel plots for FER at the normal (unpolished) carbon RCE for electrode rotation rates of: o, 0; ×, 400; *, 2500; #, 3600; O, 4900 r.p.m.

how the bubble resides on the carbon RCE at electrode rotation rates of 1000, 2500 and 3600 r.p.m., respectively, and clearly illustrate that, upon increasing the electrode rotation rate, the bubble(s) is(are) spun upward and away from the surface, leading to a smaller and smaller fraction of the surface being covered by the F_2 bubbles and, consequently, a greater surface area in contact with the melt for the FER to proceed; thus, bubble detachment is greatly facilitated by increasing electrode rotation rate at an electrode of conical configuration. However, a thin gas film may still be present on the electrode surface and may not be removable by rotation.

3.2. *Tafel plots*

Figure 3 shows the polarization behaviour (Tafel plots) for the FER at the normal (unpolished, see below) carbon RCE, in the potential range 2.0–9.0 V, for electrode rotation rates of 0, 400, 2500, 3600 and 4900 r.p.m.

The principal characteristic of these Tafel plots is their dependence on the rotation rate especially for the limiting currents at high i values which are increased (Fig. 3). Rotation of the electrodes favours F_2 evolution at substantially lower polarizations at high current densities. The limiting currents and their dependence on rotation rate are unlikely to be caused by reactant diffusion control in the electrolyte, since the experimental situation of high F^- concentration in the KF + HF mixtures used cannot (*cf.* Ref. [17]) lead to such an effect. Therefore, the results in Fig. 3 are specifically characteristic of the carbon electrode, i.e. they are determined by an effect originating probably from the abnormally high contact angle of the $C/F_2/KF \cdot 2HF$ interface [3, 4], leading to development of adherent gas films. Further examination of this point in relation to effects of polishing is given below.

The rotation dependence of bubble formation and detachment was illustrated in Figs 2a–c, and becomes significant when $i \geqslant 10^{-3}\,A\,cm^{-2}$ (see Fig. 3). This corresponds to the experimental observation that the F_2 bubble(s) become visible only when $i \geqslant 10^{-3}\,A\,cm^{-2}$. Beyond a potential of *ca* 5 V, the limiting currents that arise seem to correspond to the difficulty of bubble detachment referred to above, since the limiting currents increase markedly with electrode rotation. Thus, the presence of the F_2 bubble film is the current-restricting factor at normal carbon anodes.

Although no bubbles could be observed at the normal carbon RCE surface when the electrode was rotated at 3600 r.p.m. or more (Fig. 2d), a limiting current still arises in the high current density region of the Tafel plots (Fig. 3) under the same conditions. This result suggests that a thin F_2 gas film, in the form of bubbles of unusual lenticular form, may still be present at the RCE surface, partially disconnecting the electrode from the electrolyte and providing an extra barrier to charge transfer. At some electrodes, the presence of such a film is indicated by the metal-like reflectivity of the surface under these conditions, due to total internal reflection.

The Tafel lines in Fig. 3 for various rotation rates in the low current density range ($i \leqslant 10^{-3}\,A\,cm^{-2}$, $V \leqslant 4.0$ V) are only little dependent on electrode rotation rate and the data fall on almost straight lines with slopes of 0.4–0.5 V (this is more clearly illustrated in Figs 4 and 7 for the polished RCE). Since the bubble effect is insignificant in this range but a high Tafel slope of 0.4–0.5 V is still observed, it seems necessary to assign this behaviour to the influence of the 'CF' barrier layer film, as we and several other authors [14, 16] have suggested. The formation of such a film already over this region is indicated by the splitting of the C 1s peak in ESCA measurements as we show below in Fig. 8. However, in the higher current density region ($i \geqslant 10^{-3}\,A\,cm^{-2}$), much larger Tafel slopes arise (0.8–0.9 V), leading into the limiting currents (Fig. 3) and their observed dependence as electrode rotation rate cannot be explained only by the 'CF' film's 'barrier effect' (see discussion below). In fact, it is at these current densities of $\geqslant 0.1\,A\,cm^{-2}$, where the specially high Tafel slope of 0.8–0.9 V arises, that it is most practically important to diminish the high overvoltage that leads to the large energy consumption in industrial F_2 electrolysis.

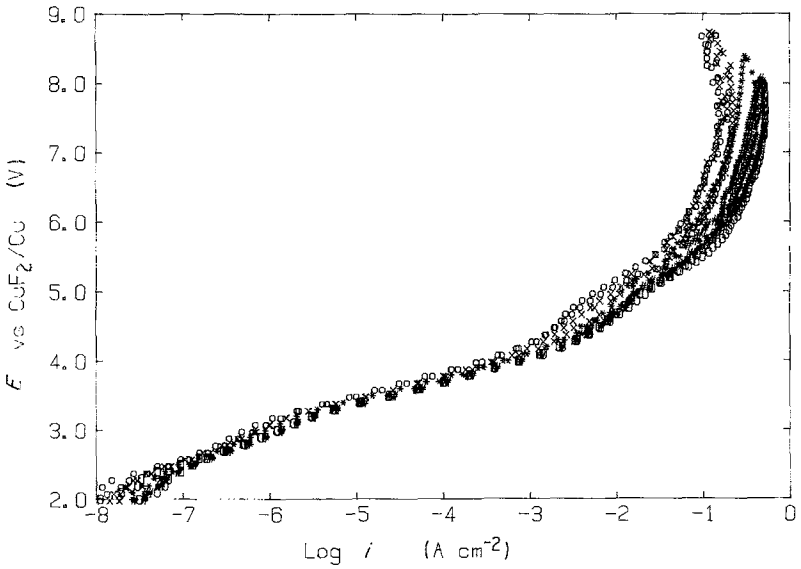

Fig. 4. Tafel plots for FER at a polished carbon RCE for electrode rotation rates of: o, 0; ×, 400; ∗, 900; #, 1600; O, 2500 r.p.m.

3.3. *Polishing effect*

The effects of polishing on the behaviour of the carbon electrodes for the FER were also investigated using a procedure patented by Eldorado Resources Ltd [11]. The polishing procedure was investigated here to establish if it has a significant effect on F_2 bubble adherence and detachment, and the associated electrode polarization.

The Tafel plots for a polished carbon RCE, determined under otherwise the same conditions as for the results in Fig. 3, are shown in Fig. 4 from which it is seen that the log i vs potential relations are much less dependent on rotation rate than are those for the normal RCE (Fig. 3). Also, for the stationary (0 r.p.m.) polished RCE much higher currents arise at given potentials (despite the external surface area per apparent cm^2 being smaller) than at the normal RCE, as illustrated in Fig. 6. In fact, for the polished stationary RCE, current densities at several potentials are comparable to those of the normal RCE only when the latter is rotated at *ca* 2500 r.p.m.

Normally, polishing an electrode diminishes the real surface area, therefore reducing the respective apparent polarization currents for the same potentials. However, in the case of the FER at carbon, since the process of F_2 bubble detachment controls the current in the high i region, removal of the F_2 bubbles is facilitated by the polishing (due to their more facile detachment) so that currents are actually increased at a given potential though the real interfacial area is diminished by the polishing.

3.4. *'Anode effect'*

Figure 3 shows that for rotation at 0 or 400 r.p.m. and for potentials $\geqslant 6$ V, the anode is passivated, i.e. the currents decrease with increasing potential and much smaller currents arise for descending than ascending directions of potential change in the polarization runs. This passivation is prevented when rotation rates are increased to > 2500 r.p.m. which strongly suggests that the 'passivation' (or so-called 'anode effect') is caused by the presence of the F_2 bubble(s), or an F_2 gas film, on the carbon electrode surface.

The relation between adherence of the F_2 bubble(s) and 'passivation' behaviour of the carbon anode is more clearly illustrated in Fig. 5 which shows plots of i vs time for a normal, stationary carbon RCE polarized at constant potentials of 6.0, 6.5, 7.0 and 8.0 V. The current is relatively stable with time when $V \leqslant 6.0$ V but it decreases with time when $V \geqslant 6.5$ V, and decreases more rapidly as the potential becomes higher.

It is interesting that, at 8.0 V for the stationary RCE (Fig. 5), the current drops from 0.26 to 0.04 A cm^{-2} within 2.5 min, i.e. the 'anode effect' had commenced and passivation had set in. However, when the 'passivated' RCE was then rotated at 3600 r.p.m., the current jumped immediately back to 0.25 A cm^{-2} and then only slowly decreased again. This result rather clearly supports the view that the 'anode effect' is caused by adherence of the F_2 bubble(s) and is not due, over the high current density range of F_2 evolution, to a surface chemical passivation effect as with anodic oxide film formation or increased 'CF' film formation as proposed in Ref. [14]. Therefore, when the RCE is rotated, causing the bubble(s) to be spun away, the current can increase rapidly again. The further slow decrease of current with time, even with the RCE being rotated at 3600 r.p.m., may be due either to formation of a very thin F_2 gas film, not in the form of bubbles, which cannot be removed even by electrode rotation, or to penetration of F_2 gas into the interior of the porous carbon.

3.5. *i vs $\omega^{1/2}$ plots*

The results of experiments at various electrode rotation rates (ω) shown in Figs 3 and 4, especially for high potentials, are represented in Fig. 6 which compares the i vs $\omega^{1/2}$ plots for the polished and normal carbon RCEs at various constant, ohmic iR corrected potentials. While it is hardly to be expected that F^- discharge from the KF · 2HF melt would be diffusion controlled, this is confirmed by the non-linear plots

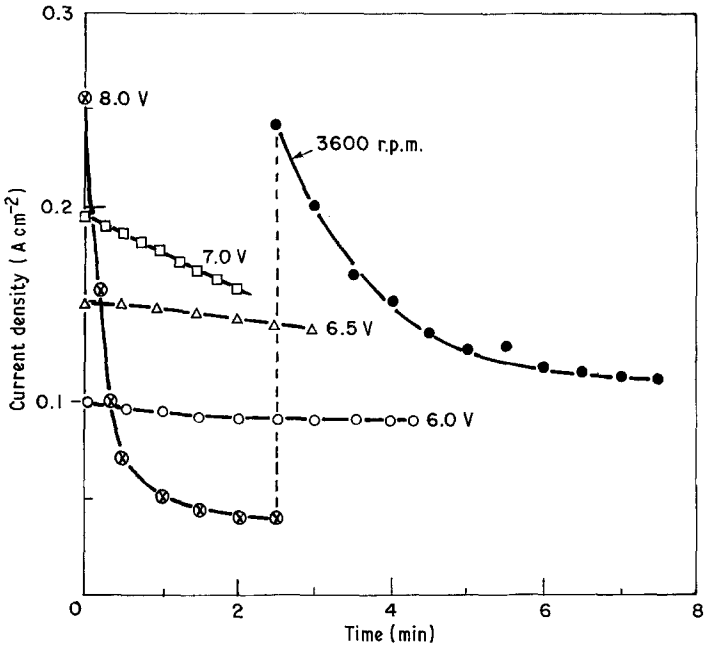

Fig. 5. Plots of i vs time for a normal carbon RCE polarized at constant potentials of 6.0, 6.5, 7.0 and 8.0 V. The RCE was kept stationary, except for the case of polarization maintained at 8.0 V for 2.4 min, following which the RCE was suddenly rotated at 3600 r.p.m.

of i vs $\omega^{1/2}$ in Fig. 6. This conclusion finds further confirmation in the fact that, over the range ω = 0–2500 r.p.m., the polished electrode passes 5–10 times higher currents than the normal electrode at the same potentials, under the same conditions (yet its roughness factor is smaller), so that the rotation dependence cannot be caused directly by a mass transport process involving the reagent ions or molecules of the electrolyte, but must arise rather from a physical process on the electrode surface.

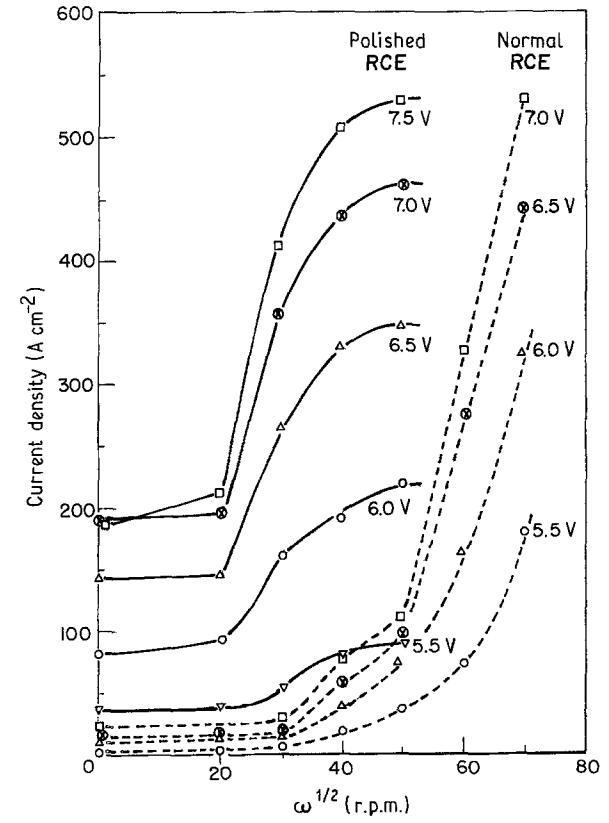

Fig. 6. Plots of i vs $\omega^{1/2}$ for the polished (solid lines) and normal (dashed lines) carbon RCEs at various constant ohmic iR corrected potentials indicated in the figure.

The plots in Fig. 6 for both types of RCEs have a flat region at the low ω ends, then i sharply increases with $\omega^{1/2}$, reaching a maximum. At the polished RCE, this increase arises already when ω = 400 r.p.m., but the maximum is not attained until ω = 2500 r.p.m., while, for the normal RCE, the sharp increase arises at ω = 2500 r.p.m. with attainment of a current maximum at 4900 r.p.m. before some decrease of current sets in at higher rotation rates (not shown in Fig. 6) due possibly to onset of turbulence.

The small increase of i from ω = 0 to 900 r.p.m. (Fig. 6) corresponds to only a small change of bubble shape (Figs 2a and b) while facilitation of detachment is observed when $\omega \geqslant$ 2500 r.p.m. (Figs 2c and d), corresponding to the sharp increase of i with $\omega^{1/2}$ (Fig. 6) when $\omega \geqslant$ 2500 r.p.m. This important effect arises evidently when the adhesive forces at the bubble/electrode/electrolyte interface are overcome by the hydrodynamic force associated with forced electrolyte flow. The above results show that this adhesion effect is smaller for the polished than for the normal RCE, as may be intuitively expected.

3.6. *Significance of high valued Tafel slopes*

The Tafel plots for polished RCEs consist of two linear regions having slopes of *ca* 0.43 and 0.88 before the currents approach limiting values (Fig. 7). For an uninhibited discharge process [9] a Tafel slope of 0.142 V (358 K) is expected if β = 0.5. In the low current density region, prior to onset of visible gas evolution, the slope is, however, 0.43 V. This high value clearly implies an inhibiting barrier effect due to a non-ohmically conducting ('CF') film ([14–16], Fig. 8). Also the more or less constant value of this slope over an appreciable logarithmic range of i implies a constant width of the barrier which is consistent with the indication [15, 16] that the 'CF' film thickness does not change much with electrode potential.

It is to be emphasized that the component of

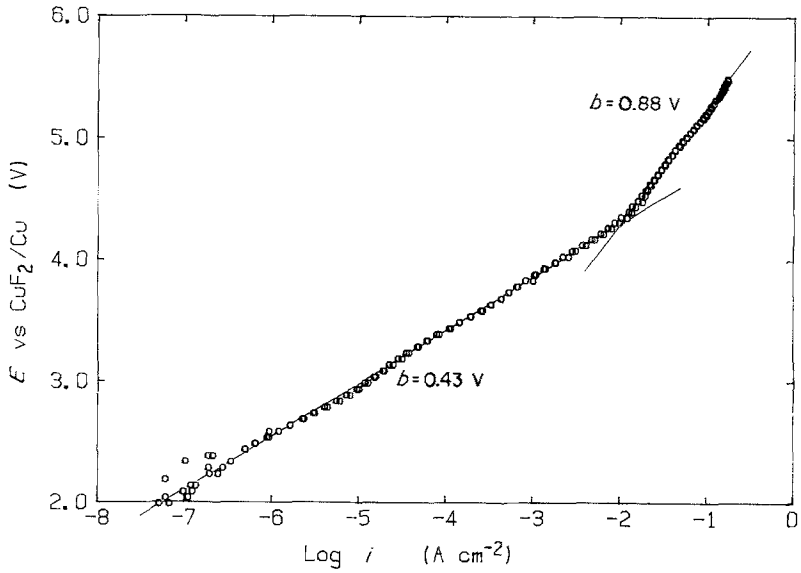

Fig. 7. Tafel plot for FER at a polished RCE (rotated at 2500 r.p.m.) before the currents approach limiting values.

polarization associated with the 'CF' film barrier effect must arise from high field, non-ohmic charge transfer behaviour so that the barrier effect is manifested as an increased Tafel slope and not simply as an '*iR*' drop effect. Thus the 'CF' film barrier effect can influence the polarization behaviour over an appreciable logarithmic range of current densities (Fig. 7), as is also found with thin oxide films in O_2 and H_2 evolution reactions at the valve metals [10].

The onset of the higher Tafel slope (0.88 V) (Fig. 7), almost twice that for lower current densities, would have to be ascribed, on the 'CF' barrier film model, to a change of film thickness; more likely is an analogous effect due to establishment of a thin gas film behaving as a barrier layer to charge transport by electron tunnelling. Probably it is this gas film barrier effect that goes over to the 'anode effect' at even higher current densities (Figs 3 and 4), giving rise to the observed limiting currents.

It may be expected that neither rotation nor polishing of the electrode should change an activation-determined Tafel slope (if such conditions change only the accessible and the real areas), but rotation could enhance the currents in the limiting current region at high current densities by bubble spin-off.

The most probable explanation of the behaviour at high current densities seems to be that the thin gas film provides an extra barrier to charge transfer, as suggested above, but this film is too thin to be spun away upon rotation. The formation and stability of the gas film, however, is intimately connected with that of the CF film, and the unusual behaviour of the former arises because of the large contact angle of the F_2/C/melt interface generated by the properties of the CF film.

As the gas film becomes thicker at high current densities, the 'anode effect' sets in and is accompanied by onset of mirror-like appearance of the electrode interface. We therefore suggest that there are really three, not unrelated, factors determining the unusual polarization behaviour of the FER at C: (i) initial formation of a 'CF' barrier film having non-ohmic charge transfer characteristics giving rise to linear logarithmic Tafel polarization behaviour but with an unusually high slope; (ii) because of this film, a high contact angle is developed between F_2 bubbles and electrolyte, giving rise to a gas film that provides an additional barrier; (iii) almost complete blocking of active electrode area at high current densities by this film, giving rise to the 'anode effect', a phenomenon to be distinguished from the unusually high Tafel slope which characterizes the polarization, due to (i), at lower current densities.

3.7. *ESCA examination of 'CF' films*

The formation of the 'CF' films on carbon anodes is indicated by splitting of the C 1s peaks of the ESCA spectra [2] shown in Fig. 8. The experimental C 1s peaks (+ points in Fig. 8) are resolvable into four components which correspond to 'C–C', 'CO', 'CF' and 'CF_2' states of C at binding energies of 284.0, 285.5, 288.2 and 291.0 eV. The area of each peak represents the relative content of each component. The broad 'CF_2' peak in Fig. 8 may consist of 'CF_2', 'CF_3', etc. surface components. Ion sputtering experiments showed the thickness of the CF film to be about 10–30 Å [15, 16]. The 'C–C' peak at 284 eV probably arises from bulk carbon atoms under the 'CF' film since the escape depth of photoelectrons from carbon is about 20–50 Å [2], taking account of the thin overlayer model [29]. More detailed discussion about these ESCA results will be given elsewhere [16].

3.8. *SEM examination of C electrodes*

SEM photos for a normal and a polished carbon electrode at the same magnification, are shown in Figs 9a and b, respectively, which indicate that the surface of the polished carbon is much smoother than that of the normal carbon, as expected.

3.9. *Test on effects of added traces of water*

Recently Nakajima *et al.* [26] found that the presence of water in a KF · 2HF melt caused the 'anode effect'

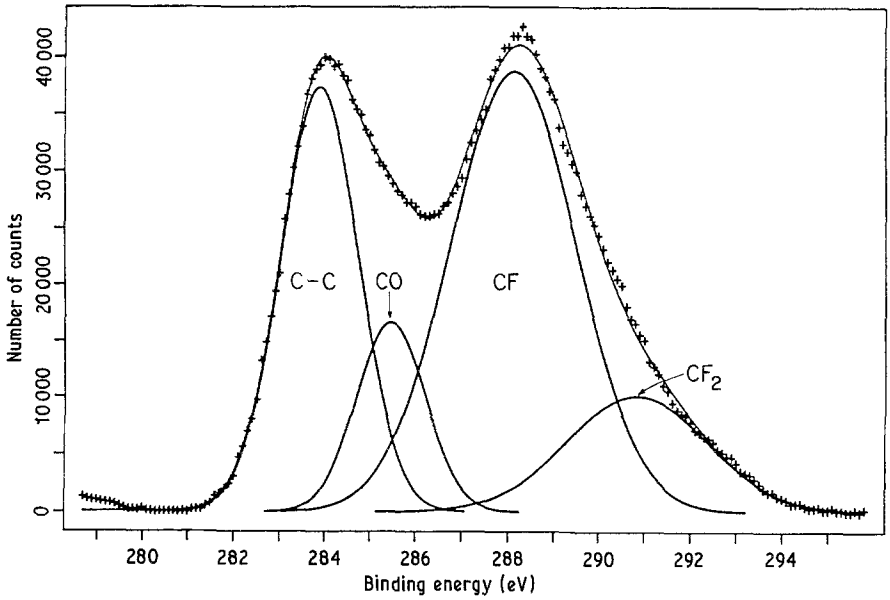

Fig. 8. The experimental (+ points) and computer-fitted and deconvoluted curves (solid lines) for detailed ESCA scan of C 1s peaks for a carbon anode after evolution of F_2.

to occur at lower current densities at a graphite electrode. On the contrary, we find that, for the regular porous carbon electrode, the presence of water in the carbon electrode could actually prevent or delay the onset of the anode effect.

The following experiment was carried out to examine the 'water effect'. Two identical carbon RCEs were prepared; one was dried at 150° C for 15 h (dry RCE), the other was soaked in double-distilled water for a few minutes and dried at 25° C for 5 min (wet RCE). Weight measurements showed that no detectable water was contained in the 'dry' RCE, while *ca* 50 mg water was present in the wet RCE.

The dry RCE exhibits a Tafel relation, with passivation ('anode effect') as the potential is taken to $\geqslant 6.0$ V (Fig. 10, curve 1). The wet RCE was first polarized at $i = 0.2\,\mathrm{A\,cm^{-2}}$ for 60 min (at *ca* 6.0 V), then a Tafel line measurement was taken, as shown in Fig. 10, curve 2. Continued measurements showed that after the wet RCE was polarized at $0.1\,\mathrm{A\,cm^{-2}}$ for 15 h, its polarization behaviour became the same as that shown as curve 1 in Fig. 10 for the dry RCE, probably on account of electrolytic removal of the water.

Figure 10 shows that the two curves are virtually coincident for $i \leqslant 10\,\mathrm{mA\,cm^{-2}}$, which suggests that water in the RCEs only affects the behaviour in the high i range, i.e. where the bubble effect is significant. Calculation shows that the extra high current at high potentials for the wet RCE is not mainly due to the anodic oxidation reaction of water itself, giving O_2, since the wet RCE only contains 50 mg water which can sustain a current of $0.2\,\mathrm{A\,cm^{-2}}$ only for less than 5 min of polarization.

The most likely explanation of the behaviour is that the presence of water in the carbon electrode changes the contact angle of the carbon/melt/F_2 gas interface, facilitating the detachment of F_2 bubbles, leading to improvement of the polarization behaviour of the RCE when wet. Another explanation, suggested by a referee, is that the water contained in the melt considerably accelerates the reaction: $C + F^{\cdot} \rightarrow CF(s) \rightarrow CF_4$, C_2F_2, etc. (see Refs [12, 28]) but it is

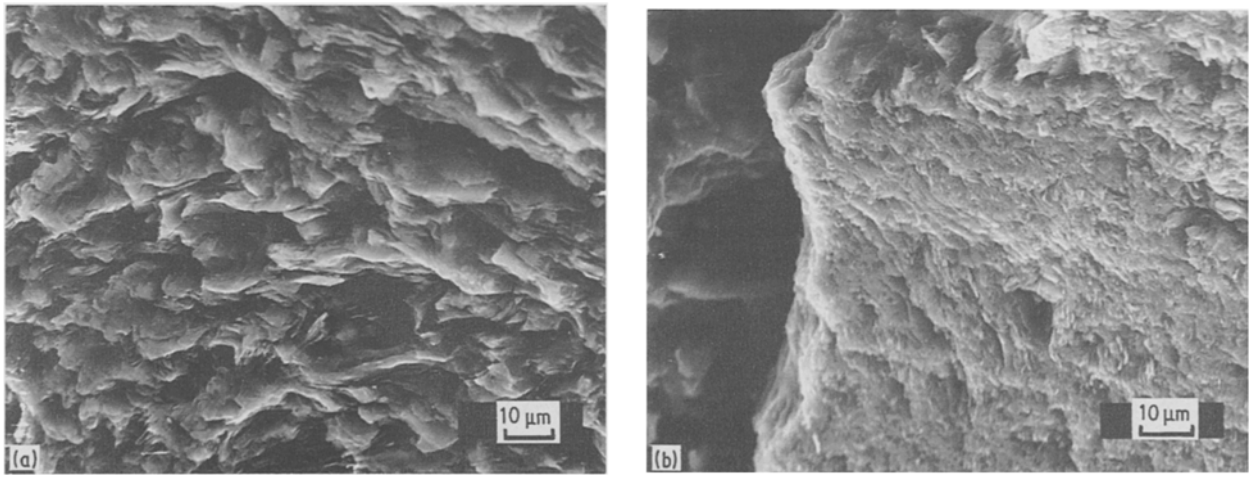

Fig. 9. SEM pictures for (a) normal, (b) polished carbon electrode at the same magnifications.

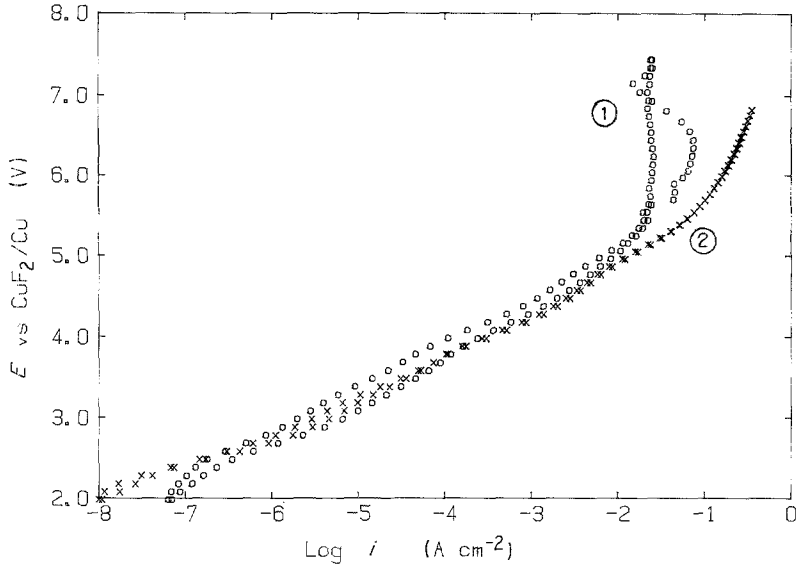

Fig. 10. Tafel plots for the FER at a dry (curve 1) and a wet (curve 2) stationary carbon RCE.

unclear why this should be so as the reactions involved are not ionic.

4. Conclusions

(i) Rotation of the carbon cone electrodes has strong effects on the FER at carbon, due to facilitation of detachment of the F_2 bubbles, which is illustrated directly by photographic studies. It is found that the formation and detachment of F_2 bubbles is the current-controlling factor in the FER at carbon anodes in the high current density range ($i \geqslant 10\,\mathrm{mA\,cm^{-2}}$).

(ii) Tafel plots for the FER at C consist of two more or less linear regions over 6–7 decades of i. At low i, $dV/d\log i$ is *ca* 0.4–0.5 V and is mainly determined by non-ohmic charge transfer through the anodically formed CF film; at high i, large values of $dV/d\log i$ arise (0.8–0.9 V) with an approach to a limiting current, and are determined by the combined barrier effect of the 'CF' film and an adherent thin F_2 gas film from which develop gas bubbles of unusual form. The latter behaviour is intimately connected with the 'CF' film formation which leads to a high contact angle at the F_2/melt/C interface.

(iii) Polishing of the carbon electrodes improves the polarization behaviour, an effect that is also mainly due to facilitation of F_2 bubble detachment.

(iv) Significant content of water in the pores of the carbon electrodes can prevent onset of the 'anode effect'. This behaviour may be also related to the F_2 bubble adherence and detachment effects.

Acknowledgement

Grateful acknowledgement is made to the Natural Sciences and Engineering Research Council of Canada and to Eldorado Resources Ltd, Ottawa, for their joint support of this research project on the P.R.A.I. program. We are also pleased to acknowledge helpful and stimulating discussions with Dr T. Zawidzki of Eldorado Resources Ltd, Ottawa, during the course of work on this project. The ESCA analysis of samples was carried out at Alcan, Kingston, by Dr D. Creber to whom we are much indebted for this contribution to the work.

References

[1] M. Chemla, D. Devilliers and F. Lantelm, Proceedings of the First International Symposium on Molten Salt Chemistry and Technology, Kyoto, Japan, April, 1983; see also D. Devilliers, F. Lantelm and M. Chemla, *J. Chim. Phys.* **80** (1983) 267.
[2] H. Imoto, T. Nakajima and N. Watanabe, *Bull. Chem. Soc. Jap.* **48** (1975) 1633; see also P. Cadman, J. D. Scott and J. M. Thomas, *Surface Sci.* **15** (1977) 75.
[3] A. J. Rudge, in 'Industrial Electrochemical Processes' (edited by A. T. Kuhn), Elsevier, Amsterdam (1971) Chap. 1.
[4] N. Watanabe, M. Ishii and S. Yoshizawa, *J. Electrochem. Soc. Jap.* **29** (1961) E180; see also N. Watanabe, 'Proc. Electrochem. Soc., Electrochemistry of Carbon' (1984) p. 536.
[5] A. J. Arvia and J. B. de Cusminsky, *Trans. Faraday Soc.* **58** (1962) 1019.
[6] N. Watanabe, M. Inoue and S. Yoshizawa, *J. Electrochem. Soc. Jap.* **31** (1963) 168.
[7] D. M. Novak and P. T. Hough, *J. Electroanal. Chem.* **144** (1983) 121.
[8] L. Bai and B. E. Conway, in course of publication (1988).
[9] J. O'M. Bockris, 'Modern Aspects of Electrochemistry' (edited by J. O'M. Bockris), Butterworths, London (1954) Vol. 1, Chap. 4.
[10] R. E. Meyer, *J. Electrochem. Soc.* **107** (1960) 847.
[11] U.S. Patent No. 4602985 to Eldorado Resources Ltd (1986).
[12] N. Watanabe, *J. Fluorine Chem.* **22** (1983) 205.
[13] M. Chemla, D. Devilliers and F. Lantelme, *Ann. Chim. France* (1984) 633.
[14] D. Devilliers, F. Lantelme and M. Chemla, *Electrochim. Acta* **31** (1986) 1235.
[15] O. R. Brown, B. M. Ikeda and M. J. Wilmott, *Electrochim. Acta* **32** (1987) 1163.
[16] L. Bai and B. E. Conway, Part II of this series, in course of publication; presented at the Conference "Centenary of the Discovery of Fluorine", Paris, August, 1986.
[17] J. S. Clarke and A. T. Kuhn, *J. Electroanal. Chem.* **85** (1977) 299.
[18] B. E. Conway and L. Bai, *J. Electroanal. Chem.* **198** (1986) 149.
[19] E. Kirowa-Eisner and E. Gileadi, *J. Electrochem. Soc.* **123** (1976) 22.
[20] N. Watanabe, S. Matsui and M. Haruta, *Denki Kaguku* **43** (1975) 638.
[21] B. Burrows and R. Jasinski, *J. Electrochem. Soc.* **115** (1968) 348.
[22] H. K. Fredenhagen and O. T. Kreft, *Z. Elektrochem.* **35** (1929) 670.
[23] C. S. Garner and D. M. Yost, *J. Am. Chem. Soc.* **59** (1937) 2738.

[24] J. Kuta and E. Yeager, 'Techniques of Electrochemistry' (edited by E. Yeager and A. J. Salkind), John Wiley, New York (1972) Vol. 1, p. 141.
[25] M. Sluyters-Rehbach and J. H. Sluyters, in 'Comprehensive Treatise of Electrochemistry' (edited by E. Yeager, J. O'M. Bockris, B. E. Conway and S. Sarangaspani), Plenum, New York (1984) Vol. 9, Chap. 4.
[26] T. Nakajima, T. Ogawa and N. Watanabe, *J. Electrochem. Soc.* **134** (1987) 8.
[27] Quarterly Report to Eldorado Resources Ltd from Electrochemistry Laboratory, University of Ottawa, March 1987.
[28] D. Devilliers, M. Vogler, F. Lantelme and M. Chemla, *Analyt. Chim. Acta* **153** (1983) 69.
[29] J. S. Hammond and N. Winograd, in 'Comprehensive Treatise of Electrochemistry' (edited by R. E. White, J. O'M. Bockris, B. E. Conway and E. Yeager), Plenum, New York (1984) Vol. 8.